Electric Parameters Determination of Solar Panelby Numeric Simulations and Laboratory Measurements during Temperature Transient

István Bodnár

Univesity of Miskolc, Faculty of Mechanical Engineering and Informatics,
Institute of Electrical and Electronic Engineering, H-3515 Miskolc-Egyetemváros,
vegybod@uni-miskolc.hu

Abstract: The efficient operation of a solar panel is influenced by several factors. Someof these factors are the intensity and the spectral composition of illumination as well as the ambient temperature together with the temperature and contamination of the solar panel and the atmosphere. This study presents the voltage, amperage, and power change of a commercially available solar panel caused by the temperature transient, by the help of numeric simulations and laboratory measurements. Temperature transient investigations allow us to know more about cooled and non-cooled solar panel behavior, in case of constant intensity of illumination. During the measurements, we have concluded that the temperature increase decreases the maximum power of the solar panel. Compared to the simulation results we experienced good tendential similarity.

Keywords: efficiency; temperature dependence; temperature transient; solar panel; simulation; laboratory measurement

1 Introduction

In today's fast-paced world, people's energy consumption has become enormous. Over the last century, the energy demand of an ordinary person has grown by about fivefold, which is attributed to the spread of machinery and electronics. In order to avoid the excessive consumption of our energy carriers, both in energy production and consumption the increase of efficiency became important. The operating efficiency of the solar panel is influenced by the installation environment and the weather conditions. Among these factors, the intensity of illumination, the temperature of the solar panel's surface and its ambient temperature together with the surface pollution of the solar panel and its shadow effect are the most significant. During the research, I present the effect of solar panel surface temperature on its electrical parameters.

I. Bodnár

Electric Parameters Determination of Solar Panel by Numeric Simulation
and Laboratory Measurements during Temperature Transient

The main goal of the research is to establish a correlation between the surface temperature of the solar panel and its electrical parameters. The correlations were determined by laboratory measurements and numerical simulations.

Numerous literature deals with measurements and simulations at constant temperatures, but the present paper contains measured and simulated results in the transition state, which is the novelty content of the research work.

2   The Operation of Solar Panel

To understand the operation of solar panel, we examine a p-n junction semiconductor cell, which is the base of most solar panel constructions. If the energy of photons, coming from the sun is higher than the E_g , energy of the prohibited line, photons generate electron-hole pairs. The voltage, generated inside of the p-n junction disparts the electrons and holes and also prevents the recombination. Electrons move toward to the n-side, while holes move toward to the p-side. So if the energy of photons is high enough, then a so-called photo-current appears inside of the solar panel. This generated photo-current flows in the same direction as the dark current [1].

During the process we can measure the Open Circuit voltage (U_{OC}) between the poles of the solar panel and in case of shorting the solar panel, the Short Circuit current (I_{SC}) too. If we connect electrical load to the solar panel, we experience U voltage and I current, which are always lower than the U_{OC} and I_{SC}, measured in case of an unloaded solar panel. The I current is the difference between the I_{ph} photocurrent and I_D diode current, which is described by *Formula 1*. [1, 5, 9]:

$$I = I_{ph} - I_D = I_{ph} - I_s \left[exp \left(\frac{eU}{kT} \right) - 1 \right]. \tag{1}$$

The I_D diode current can be defined by the help of the I_s diode saturation current, depending on the voltage and constants.

The simplified electronic model of the solar panel, ignoring all the resistive and capacitive natured elements, consists of a diode and a current generator. The produced current of the current generator depends on the intensity of illumination [5, 12, 13]. *Figure 1*. contains this model together with the mentioned I, I_D, I_{ph} current directions.
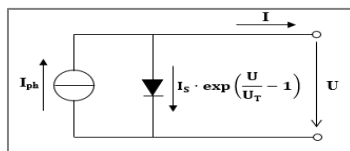

Figure 1

Model of the ideal, unloaded solar panel

By substituting $U=0$ and $I=0$, the short circuit current (2) and the open circuit voltage (3) can be defined easily [5, 9, 10, 12, 13]:

$$I_{SC} = I_{ph}, \tag{2}$$

$$U_{OC} = \frac{k \cdot T}{e} \cdot ln\left(\frac{I_{ph}}{I_s} + 1\right) = U_T \cdot ln\left(\frac{I_{ph}}{I_s} + 1\right), \tag{3}$$

where: $U_T = \frac{k \cdot T}{e}$ the thermic voltage.

It can be seen that the short circuit current is directly proportional to the strength of illumination, as the photocurrent increases with the light intensity increase and *Formula 2.* shows that the photocurrent equals to the short circuit current. From *(3)* we can see that the open circuit voltage logarithmically depends on the light intensity, measured on the surface and is directly proportional to the thermic voltage. The U_T thermic voltage represents the voltage change caused by the temperature. By knowing the open circuit voltage and the short circuit current, the *U-I* graph can be drawn. *Figure 2.* shows the *U-I* characteristics in case of different light intensities. It can be seen that if the intensity decreases, the short circuit current decreases much more than the open circuit voltage. Therefore, we can say that the intensity does not affect the open circuit voltage as it only decreases by a few Volts [1, 5, 9, 10, 12, 13].
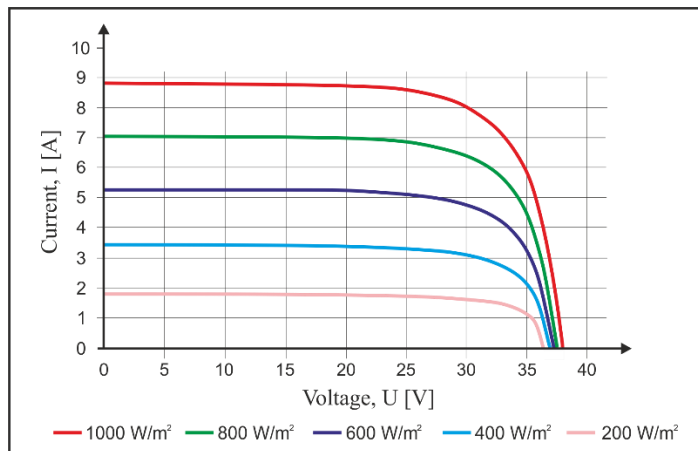

Figure 2
The U-I curves of the solar panel in case of different light intensities

In the following, consider the electric model of the solar panel without neglecting the losses. Both internal and wire resistance is represented by an ohmic resistance in this case. A capacitor can also be connected in parallel to the diode, representing the parasitic capacitance between the two poles of the diode, but because of its value, it is negligible. According to these, the mentioned equations need to be modified. *Figure 3.* shows this model [1, 5, 12, 13, 33].
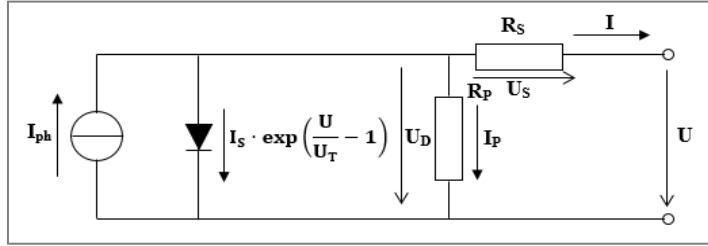
Figure 3

The real circuit model of the solar panel

This more realistic model modifies the equations too. The currents and voltages are the following [5, 9, 10, 12, 13, 33]:

$$I = I_{ph} - I_D - I_P, \tag{4}$$

$$I_D = I_s \left[exp\left(\frac{e \cdot U_D}{n \cdot k \cdot T \cdot N_S} \right) - 1 \right], \tag{5}$$

$$I_P = \frac{U_D}{R_p} = \frac{U + I \cdot R_S}{R_p}, \tag{6}$$

$$U = U_D - U_s. \tag{7}$$

Ideally $R_p \approx \infty$ and by shorting the circuit means: $R_D \gg R_s (R_{Cp} \gg R_s)$ [5].

3 Mathematical Determiantion of Solar Panel's Electrical Parameters

3.1 Power of the Solar Panel

The efficient P power of the solar panel can be counted by the multiplication of the I amperage and U voltage, measured on the R resistance. According to the simplified model [5, 7, 33]:

$$P = I \cdot U = I_{SC} \cdot U - I_s \cdot U \cdot exp\left(\frac{U}{U_T} - 1 \right). \tag{8}$$

The maximum power of the solar panel can only by reached if we suit the load resistance. To find the extreme value of relation *(8),*we partially derive the function by U and look for the solution of the $\frac{\partial P}{\partial U} = 0$ equation. From this, the amperage *(9)* and the voltage *(10)* of the operating point can be expressed, while producing the maximum power [5, 7, 9, 10, 12, 13, 33].

$$I_M = I_{ph} - \frac{U_M}{U_T} \cdot I_s \cdot exp\left(\frac{U_M}{U_T} \right) \approx I_{ph} \cdot \left(1 - \frac{U_T}{U_M} \right), \tag{9}$$

$$U_M = U_{OC} - U_T \cdot ln\left(1 + \frac{U_M}{U_T}\right). \tag{10}$$

The value of the optimal R_M load resistance can be determined *(11)* according to Ohm's law, from equation *(9)* [5, 9, 10, 12, 13, 32, 33]:

$$R_M = \frac{U_M}{I_M} = \frac{U_T}{I_s \cdot exp\left(\frac{U_M}{U_T}\right)} = \frac{U_T}{I_M + I_s + I_{ph}}. \tag{11}$$

The ideal value of the load resistance equals to the internal resistance of the solar panel. If this is true in practice, then the solar panel is operating in maximum power point (MPP) [5, 7]. The maximum power point can be found with the help of a maximum power point control unit. MPPT controllers use different algorithms, the two main types of which are True Maximum Point Seeking (TMPS) and Non-true Maximum Point Seeking (NMPS) maximum point seekers. The most common are the climbing and oscillating algorithms. To achieve maximum power, the load on the solar panel must be changed dynamically. Similar algorithms are used by Precup et al.[22] and Ürmös et al. [23] and Shams et al. [24].

The so-called φ fill factor shows how the multiplication of U_M voltage and I_M amperage of the operating point relates to the multiplication of U_{OC} open circuit voltage and I_{SC} amperage *(12)* [5, 7, 14, 17, 32]:

$$\varphi = \frac{P}{P_{th}} = \frac{U_M \cdot I_M}{U_{OC} \cdot I_{SC}}. \tag{12}$$

We can see in *Figure 4.,* how the rectangle area of the maximum power (grey rectangle, $I_M \cdot U_M$) relates to the theoretical power (multiplication of $I_{SC} \cdot U_{OC}$) determined rectangle area [12, 13, 14, 32, 33].
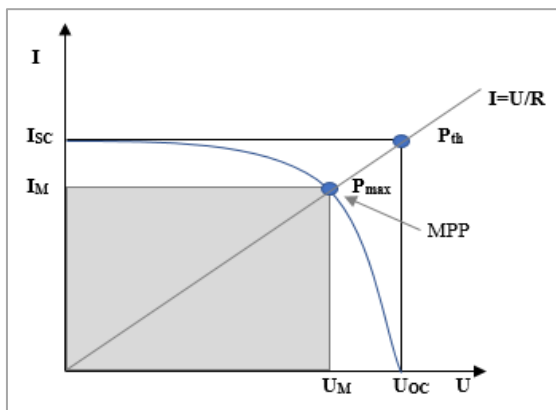

Figure 4
The operating point of the maximum power on the U-I curve

The value of the φ fill factor depends on the structure of the solar panel and on the chosen operating point. The value of φ, in case of solar panel used in practice is

between 0.75 and 0.85. However, its value significantly decreases during its aging. The older the solar panel, the lower the value of the fill factor is, which results in a reduction of efficiency [5, 7, 9, 10, 32].

3.2   The Efficiency of the Solar Panel

The maximum power point efficiency η_{max} of the solar module can be counted by dividing the P_{max} maximum power of the solar panel with the P_{light} light power, measured on the effective surface *(13)* [6, 14, 15, 16, 27, 32, 33]:

$$\eta_{\max}(T) = \frac{P_{max}(T)}{P_{light}} = \frac{I_M \cdot U_M(T)}{P_{light}} = \frac{\varphi \cdot P_{th}(T)}{P_{light}} = \frac{\varphi \cdot I_{SC} \cdot U_{OC}(T)}{P_{light}}. \tag{13}$$

Since the power output of the solar panel is dependent on the temperature, its efficiency is also a function of temperature. The function has a maximum that gives the maximum efficiency of the solar panel. It should be noted here that the solar panel operates with maximum efficiency when the intensity of illumination is low and its temperature is colder [28, 39]. The maximum power and maximum efficiency at the same time can be guaranteed if the solar panel is cooled during the operation while the load is dynamically optimized. Guo et al. [37] and Farshchimonfared et al. [38] shows opportunities for this purpose, where they combine solar panels with solar collectors.

The energy magnitude of the prohibited band E_g is an important parameter during the determination of the solar panel's efficiency. If the energy of the incoming photon E_{photon} is lower than the energy of the prohibited band, then the potential electron is not able to leave the valence band and to enter the conducting band, so photocurrent can not be formed. Therefore, the creation of prohibited band width above the photon's energy is necessary to generate charge carriers. The extra energy (E_{foton} - E_g) transforms into heat [4, 5, 28].

3.3   The Effect of Temperature and Intensity on the Current and Voltage

The T_S operating temperature of the solar panel can be expressed by equation *(14)*:

$$T_S = (T_N - T_A) \cdot \frac{E_{ill}}{E_{STC}} + T_A, \tag{14}$$

where: T_N – the nominal temperature of the solar panel (K),
       T_A– the ambient temperature (K),
       E_{ill} – the intensity of illumination (W/m^2) [3, 4, 17, 18, 26].

Taking these into account, the photocurrent can be determined as a function of temperature [3, 4, 17, 18, 25, 26, 33]:

$$I_{ph} = I_{SCN} \cdot [1 + \mu_{ISC} \cdot (T_S - T_A)] = I_{SCN} + K_{ISC} \cdot (T_S - T_A), \tag{15}$$

where: μ_{Ir} – the percentage coefficient of the short-circuit current (%/K),

K_{ISC} – the coefficient of the short-circuit current (A/K),

$E_{int\,standard}$ – the intensity of standard illumination (1.000 W/m^2).

If the intensity also changes, the photocurrent value can be written as follows [3, 4, 17, 18, 25, 26, 33]:

$$I_{ph} = \frac{E_{int}}{E_{int\,sztenderd}} \cdot I_{SCN} \cdot [1 + \mu_{Ir} \cdot (T_S - T_A)] =$$

$$\frac{E_{int}}{E_{int\,sztenderd}} \cdot I_{SCN} + K_{ISC} \cdot (T_S - T_A). \tag{16}$$

According to *correlation (16),* the intensity of the illumination and the temperature change also linearly influence the amperage. It can be concluded that if the intensity of the illumination and/or the temperature of the solar panel increases, the voltage drops, so the efficiency of the solar panel decreases.

The saturation current value, as a function of temperature can be calculated based on the two diode models [3, 4, 9, 10, 12, 13, 17, 18, 25, 30, 33]:

$$I_S = \frac{I_{ph}}{\left[exp\left(\left(\frac{e \cdot U_{OC}}{n \cdot k \cdot T \cdot N_S}\right) \cdot (1 + \mu_{UOC} \cdot (T_S - T_A))\right)\right] - 1}, \tag{17}$$

where: μ_{UOC} – the percentage coefficient of the idling voltage (%/K).

The temperature dependence of idle voltage [3, 4, 17, 18, 25, 26, 33]:

$$U_{OCT} = U_{OCN} \cdot [1 + \mu_{UOC} \cdot (T_S - T_A)] = U_{OCN} + K_{UOC} \cdot (T_S - T_A), \tag{18}$$

where: K_{UOC} – the coefficient of idle voltage (V/K).

The power of the solar panel and its efficiency can be determined by the voltage. Amperage can be determined depending on the power (8) and efficiency (13) of the solar panel. All the results of the literature show that the increase in both the temperature and the intensity of illumination results in a decrease in the efficiency of the solar panel [8, 11].

4 The Measurement Compilation and Description of the Measuring Process

4.1 The Sun Simulator

The design of the appropriate lighting conditions was a very important part of constructing the measuring compilation. Simulating the light of nature is an extremely difficult task. Attention should be paid to the intensity of the light, the uniformity of its distribution and to the similarity of the light spectrum of the

I. Bodnár

Electric Parameters Determination of Solar Panel by Numeric Simulation
and Laboratory Measurements during Temperature Transient

illumination and sunlight. According to the *IEC 60 904-9* (Sun Simulator Performance Requirements) the lighting can be classified into different classes according to the homogeneity of the light intensity distribution. For the worst, C-type devices, the ± 10% difference is allowed. Thus, based on the naturally occurring maximum 1,000 *W/m²* light intensity, the value of light intensity can move between 900−1,100 *W/m²* with standard illumination [19, 20, 26]. The reflectors at my disposal did not allow me to meet the criteria prescribed by the standard Therefore, spectral energy density divergences were taken into account by a constant factor. At present, I am working on developing a new kind of simulator for accurate measurements. The intensity distribution of the Sun simulator is shown in *Figure 5*.
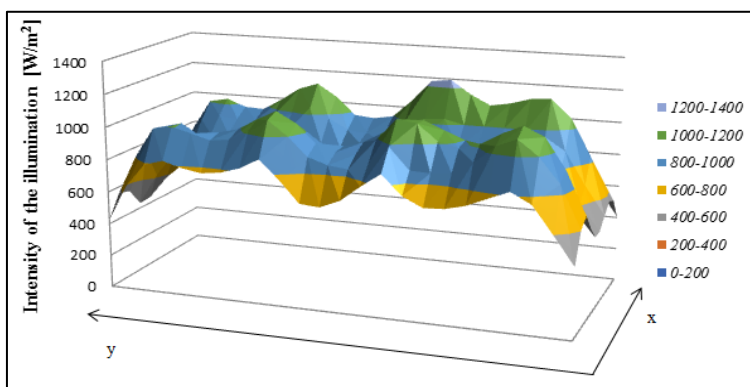

Figure 5
Reflector layout with the associated light intensity distribution

The inhomogeneity of illumination is described in (19) [21]:

$$\Delta E = \frac{E_{max} - E_{min}}{E_{max} + E_{min}} \cdot 100\%, \tag{19}$$

where: ΔE− the degree of inhomogeneity of the illumination [%];

E_{max}− the maximum light intensity value $\left[\frac{W}{m^2}\right]$;

E_{min}−the minimum light intensity value $\left[\frac{W}{m^2}\right]$.

In the measurement setup: E_{max} = 1,245 *W/m²*, E_{min} = 407 *W/m²* and *ΔE* = 50.73%. The median: 874 *W/m²*, the modus: 1,000 *W/m²*. The light power is: 490.48 *W*.

The significant inhomogeneity determined on the basis of (19) is caused by the drastic reduction of the light intensity on the corners of the illuminated surface. However, if we look at the light intensity distribution shown, it is clear that this surface is a very small fraction of the effective surface. Therefore, the homogeneity of the light intensity distribution is more satisfactory for the remainder of the solar panel.

The value of the average light intensity per solar panel (integrated mean value) can be calculated by means of *formula (20)* from the previously determined real light intensity distribution matrix elements [19].

$$E_{average} = \left(\sum_{i=1}^{10} \sum_{j=1}^{24} (E_{ij} \cdot A_{cell})\right) \cdot \frac{1}{A_{solar\,module}}, \tag{20}$$

where: $E_{average}$–the value of the average light intensity per solar panel W/m^2;

  E_{ij}–the value of the light intensity per cell W/m^2;

  A_{cell}– area of one cell (A_{cell} = 0.0025 m^2);

  $A_{solar\,module}$–the size of the solar panel's surface ($A_{solar\,module}$ = 0.5695 m^2).

In the measurement setup: $E_{average}$= 861.267 W/m^2. This is slightly below the maximum 1,000 W/m^2 in nature. This light intensity value corresponds to the value of light intensity on a slightly cloudy day. However, due to the shift of the spectral energy of the halogen reflector from the natural light, according to the Vienna law, we have to consider a constant [8, 11, 19, 26, 28]. *Figure 6.* illustrates different light source spectral compositions. It can be observed that the spectral composition of the Sun simulator used differs significantly from the sunlight's.
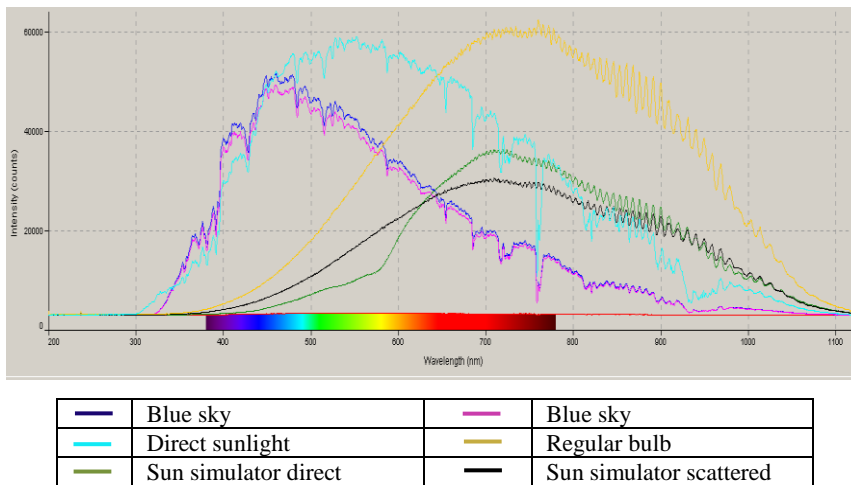

	Blue sky		Blue sky
	Direct sunlight		Regular bulb
	Sun simulator direct		Sun simulator scattered

Figure 6

Spectral composition of different light sources

4.2   The Compiled System and its Components

For the measurements, I used a KS-85 monocrystalline solar panel, created by korax solar. The solar panel was placed on a same sized table az its own size, and 50 *mm* thick wooden slats were placed under the solar panel to lift it, and to create a flow channel between the back of the solar panel and the table. The cool air, to cool the solar panel, was given by an *Orion CSHP 9001 C4* typed mobile climate system. The cold air outflow from the climate was driven by a plastic film to the

I. Bodnár

Electric Parameters Determination of Solar Panel by Numeric Simulation
and Laboratory Measurements during Temperature Transient

already mentioned flow channel. This plastic film worked as a buffer and made the flow sufficiently even. Preliminary temperature examinations proved that the reverse side of the solar panel heats up the same as the absorber surface. According to these, it is possible to withdrawal thermal energy from the reverse side of the solar panel too, so this kind of cooling proved to be functional. The basic assumption is that applying a cooling system increases the power of the solar panel. The compiled system can be seen in *Figure 7*.

Figure 7
The measurement layout

A *YC-747D* typed, four channel digital thermometer was applied to measure the temperature of the solar panel. The four sensors were placed to different parts of the solar panel (Figure 8). in the following, the average temperature of the four points was considered to be the temperature of the solar panel. The sensors were fastened to the surface of the solar panel by the use of good thermal conductive aluminum tape to ensure the accuracy of the results, making sure that the shielded surface is negligibly small.

The temperature of the illuminated and non-cooled solar panel reached 80 *°C*. With applying this cooling, I was able to decrease this temperature by 15 *°C*. To further cool, I tried to extract heat from the absorber surface of the solar panel with the use of a *TT 150* type pipe fan. The flow channel between the reflector and the fan was also created by using plastic film. This solution widened the flow area, so a larger surface of the solar panel could be cooled. It is important to mention that this solution decreases the speed of the flow. When the air conditioner and the fan were used together, the average temperature of the solar panel had decreased by 40 *°C*. Then, the air flowing out of the fan outlet was directed to the surface of the solar panel, so I did not use the previously mentioned deflector. In this case, the speed of flow did not decrease and a further 10 *°C* decrease was achieved. So

using both the climate system and the fan this way means a 50 *°C* temperature decrease. The average temperature in this case was 30 *°C.*

Figure 8
Placing the four sensors on the absorber surface on the solar panel

The load resistance of the solar panel was modelled by a high powered potmeter. The resistance of this potmeter could be set between 0.7 and 7.2 Ω, according to measurements. I used a *Protek DM-301* and a *METEX M-365OD* type digital multimeter to measure the voltage and amperage of the solar panel at the same time.

The purpose of the measurement was to find out the processes during temperature transient. According to the literature, it can be said that the open circuit voltage of the solar panel decreases significantly, while its short circuit amperage slightly increases by the temperature increase. The voltage decreases more than the amperage increases, so the power of the solar panel decreases too in case of higher temperature.

4.3   Constants and Baseline Data Considered during the Simulation

The numerical simulations were made using the equation system of the two-diode model mentioned in the previous chapters. During the simulation, I started from the simplified circuit model of the solar panel. Table 1 contains the constants used during the simulation, while the electrical parameters of the solar panel can be seen in Table 2.

Table 1

Constant parameters [5, 19, 20, 25, 30]

Parameter	Symbol and measurements	Value
The solar irradiation intensity at standard test conditions	E_{STC} [W/m^2]	1,000
Intensity of illumination	E_{ill} [W/m^2]	861
Diode reverse bias saturation current (according to the two diode model)	I_s [A/cm^2]	$1 \cdot 10^{-11}$
Electron charger	e [C]	$1.60 \cdot 10^{-19}$
Boltzmann constant	k [J/K]	$1.38 \cdot 10^{-23}$
Diode ideality factor	n [-]	2
Constant of the light spectral composition	C [-]	0.532

Table 2

Electrical parameters of the solar panel

Parameter	Symbol and measurements	Value
Year of manufacture	-	2008
Peak Power	P_{max} [W]	85
Max. power current	I_M [A]	4.88
Max. power voltage	U_M [V]	17.45
Short circuit current	I_{SC} [A]	5.40
Open circuit voltage	U_{OC} [V]	21.20
Nominal fill factor	φ [-]	0.74
Serial resistance	R_s [Ω]	0.0035
Parallel resistance	R_P [Ω]	10,000
Number of serial connected cells	N_S [piece]	18
Number of parallel connected cells	N_P [piece]	2
Temperature co-efficient for P_{max}	K_{PM} [W/°C]	-0.391
Temperature co-efficient for I_{sc}	K_{ISC} [A/°C]	0.001674
Temperature co-efficient for U_{oc}	K_{UOC} [V/°C]	-0.073776
Percentage Temperature co-efficient for P_{max}	μ_{Pm} [%/°C]	-0.460
Percentage Temperature co-efficient for I_{sc}	μ_{Isc} [%/°C]	0.031
Percentage Temperature co-efficient for U_{oc}	μ_{Uoc} [%/°C]	-0.348
Efficiency (maximal power)	η [%]	12.75
Nominal operating temperature	T_N [°C]	25

During the simulation, I had the following considerations and ommisions:

- I reduced the solar module to one cell,
- I omitted the serial and parallel resistance,
- I took the integrated mean of the intensity of the illumination,
- I calculated with the help of the open circuit voltage, short circuit current and temperature constant, which were given by the manufacturer,
- I considered the difference between the spectral composition (spectral energy density) of the halogen and the sunlight as a constant [5, 9, 10, 12, 13, 25].

4.4 The Modified Model

The modified model uses the temperature constants, determined with the help of the measurement results. It does take the open circuit voltage and short circuit current, given by the manufacturer into account. The temperature constant from the measurements are given in Table 3.

The simulation with the modified model aims to estimate the deterioration of efficiency, caused by the aging of the solar panel. Aging examinations provide more accurate data if the intensity is constant and the temperature is varied. The measurements should be done at different intensities and then average the results with statistical methods.

Table 3

Thermal constants derived from the measurements

Parameter	Symbol and measurements	Value
Temperature co-efficient for P_{max}	K_{PM} [W/°C]	-0.5255
Temperature co-efficient for I_{sc}	K_{ISC} [A/°C]	0.000594
Temperature co-efficient for U_{oc}	K_{UOC} [V/°C]	-0.08692
Percentage Temperature co-efficient for P_{max}	μ_{pm} [%/°C]	-0.459
Percentage Temperature co-efficient for I_{sc}	μ_{Isc} [%/°C]	0.011
PercentageTemperature co-efficient for U_{oc}	μ_{Uoc} [%/°C]	-0.410

Table 4

The ratio of theoretical (catalogue) and counted (measured) temperature constants

	Catalog$\left[\frac{\%}{°C}\right]$	Measurement$\left[\frac{\%}{°C}\right]$	Ratio[%]
μ_{pm}	-0.46	-0.459	99.78
μ_{Isc}	0.031	0.011	35.48
μ_{Uoc}	-0.348	-0.41	117.82

Thermal constant of the open circuit voltage, derived from the measurements approximates the value given by the solar panel manufacturer. This proves the accuracy of my measurement. The deviation may be caused by the inaccuracy of the measurement and the aging of the solar panel may also affect this value (the year of manufacture of the solar panel I used was: 2008).

Instead of this, the value of the thermal constant of the short circuit current differs greatly from the catalog data. This may by caused also by the inaccuracy of the measurement and the properties of the illumination because the light conditions produced in my case were not the same as those that were used during the qualification of the solar panel. If we consider the difference of the illumination's spectral composition, then the thermal constant of the short circuit current from the measurement results is 0.0207 %/°C, which means 66.77% of the one, which is given by the manufacturer.

5   Comparasion ofMeasurement and Simulation Results

5.1   Transient Examination in Case of Unloadid Solar Panel

I made transient examinations by using an unloaded solar panel at first. In this case, I turned the illumination and the cooling system at the same time. I measured the temperature at four places in every minute for 20 minutes. I also measured the open circuit voltage, generated by the cells, and the short circuit current (Section 1). After this, I turned the cooling system off, and resumed sampling at 10 measuring points for 10 minutes (Section 2). After the solar panel temperature stabilized, it had been cooled down to the initial temperature, by inserting the previously described cooling fan (Section 3). The temperature-time graph is shown in Figure 9. It can be observed that the surface temperature of the solar panel changes exponentially while applying the cooling system. I show the results as a function of the temperature, however, a scale still indicates a lapse of one minute, so the temperature and time function can be written simultaneously.

Without cooling, the temperature of the solar panel, determined by the average of the four sensors, seemed to remain constant at 74.88 °C. The temperature, defined by equation (14) is 76.66 °C, so the value is 2.38% higher than the measured value.
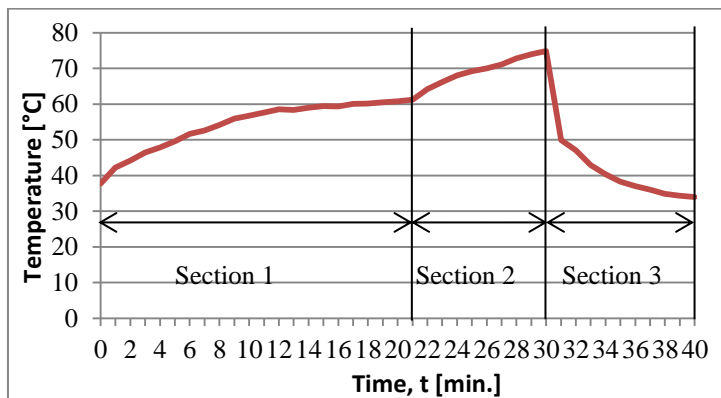
Figure 9
The time function of the temperature of the solar panel's surface

The short circuit current value, as a function of the temperature can be seen in Figure 10. It can be observed that the current-temperature (time) curve outline in the measurement results follows the curve outlined on the basis of numerical simulations based on catalog data. The time-averaged difference is 4.14%, while the difference created with the help of the modified model is 1.38%. So the modified model gives a more accurate approximation overall, but the outlined curve is less similar to the measured curve. For each curve it can be said that depending on the temperature, the expected amperage-change occurred. The amperage increased without cooling, while it decreased with cooling. The same tendency can be seen in some similar publications, such as Singh et al. [28] and Malik et al. [31].

The temperature dependence of the open circuit voltage can be seen in Figure 11. It can be noticed that the modified model had produced nearly coincident results with the measured results during lightly cooling the solar panel. The model is more similar to the basic model in the case of non-cooling or strong cooling. The modified model overestimates the measured results in time-average by 2.52%, while this percentage is 5.98%, in case of the basic model. These results are very similar to the results which were obtained by many other studies, such as Singh et al. [28], Chantana et al. [29] and Malik et al. [31].
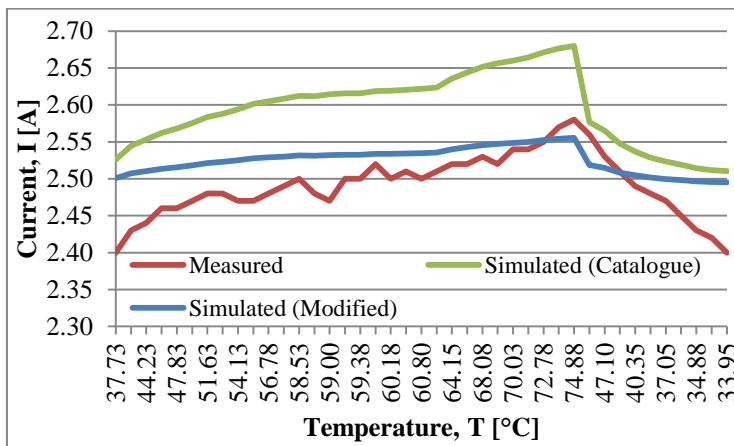
Figure 10

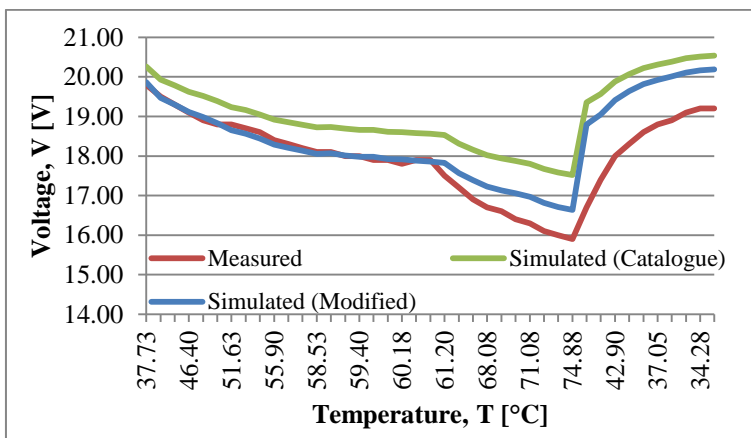The short circuit current of the solar panel, depending on the temperature (time)

Figure 11

Temperature (time) dependence of the solar panel's open circuit voltage

The theoretical power graphs can be seen in Figure 12. It can be clearly stated that the theoretical power decreases due to the increase in the solar panel's temperature. This was assumed, based on the theoretical power calculation (1). The reason of the decrease is that the voltage of the solar panel decreases more than its amperage increases with the temperature increase. The simulation basic model estimated the theoretical power by 10.34%, while the modified model estimated it by 3.92%.

Based on numerical simulations using catalog data, it can be said that the theoretical power (and efficiency) of the solar panel 9.32%, while in case of the simulation with the modified model is 3.7% less than in case of its new state. The

modified model calculates with temperature constants determined from the measurement results, but it considers the open circuit voltage and short circuit current, given by the manufacturer. Therefore, the decrease in power caused by the aging of the solar panel can be attributed to this value. The 3,7% drop in power and efficiency deterioration can approximate better the real value.

Overall, it can be said that the temperature increase causes a decrease in the open circuit voltage, while the short circuit amperage only slightly increases, and the multiplication of these amounts, so the power of the solar panel decreases too. In the reverse case, if the solar panel cools down, the voltage and the power increases, while the amperage decreases. The experiments proved that the phenomenon, described in the literature is correct.
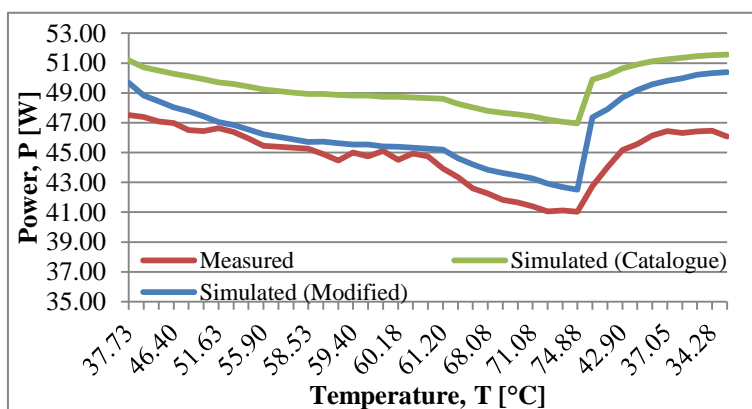

Figure 12
Temperature (time) dependence of the solar panel's theoretical power

Table 5 summarizes statistical data for differences between simulation and measured results, during transient analyzing in the case of an unloaded solar panel. It can be observed that the largest difference between simulation and measurement of open circuit voltage and theoretical power is greater than 10% for both the catalog and the modified model. There is no repeat (modus) in the deviations.

Table 5
Statistical data for the difference between the simulated and measured results.

	Simulated (Catalog)				Simulated (Modified)			
	Min [%]	Max [%]	Median [%]	Avarage [%]	Min [%]	Max [%]	Median [%]	Avarage [%]
I_{SC}	0.66	5.84	4.59	4.14	-1.71	4.20	1.31	1.38
U_{OC}	2.20	15.92	4.52	5.98	-0.87	12.58	0.63	2.52
P	6.60	16.68	9.91	10.34	0.66	10.77	2.93	3.92

I. Bodnár

Electric Parameters Determination of Solar Panel by Numeric Simulation
and Laboratory Measurements during Temperature Transient

5.2   Transient Examination inCase of Loaded Solar Panel

Temperature transient analyzes were made in case of a loaded solar panel in two cases. I connected a 4.2 ohm resistor to the terminals of the solar panel. In the first case, the solar panel was non-cooled, while in the other case the cooling was continuous. I measured the terminal voltage, the amperage and the temperature of the solar panel every minute. The purpose of this measurement was to reveal the change in electrical parameters of a chilled and a non-cooled solar panel, operating at the same temperature. The temperature-time curves in both cases can be seen in Figure 13. It can be observed that the temperature in both cases increased by time.
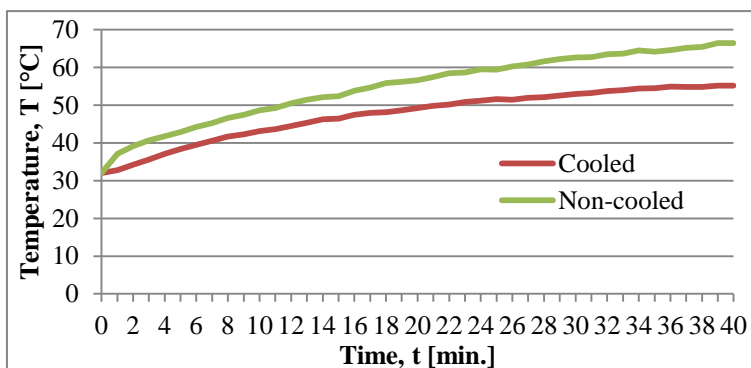

Figure 13

The time function of the temperature of the loaded solar panel's surface in chilled and non-cooled cases

Figure 14. shows the amperage. In both the simulations and the curves from the measurement it can be seen that with time (temperature increase) the chilled and non-cooled curves are merged. The time-average difference between the simulation and the measurement results for the chilled solar panel is 2.67%, and this is 3.85% without cooling. Many other researchers received similar results, for example Singh et al. [28] and Malik et al. [31].

In Figure 15 the voltage, as the function of time (temperature) can be seen. It can be observed in both the simulation and the measurement results, the curves of the chilled and non-cooled solar panel cross each other, just like in case of other researches: Singh et al. [28],Chantana et al.[29] and Malik et al. [31]. The time-averaged difference in cooled case is 4%, while without cooling it is 4.03%.

Figure 16 shows the power of the solar panel. It can be seen, that the curves from the simulation and measurement show the same characteristics. The characteristics of both the chilled and the non-cooled solar panel cross each other in case of simulation and measurement too. The time-average difference in case of cooled solar panel is 6.79%, while it is 8.04% without cooling.
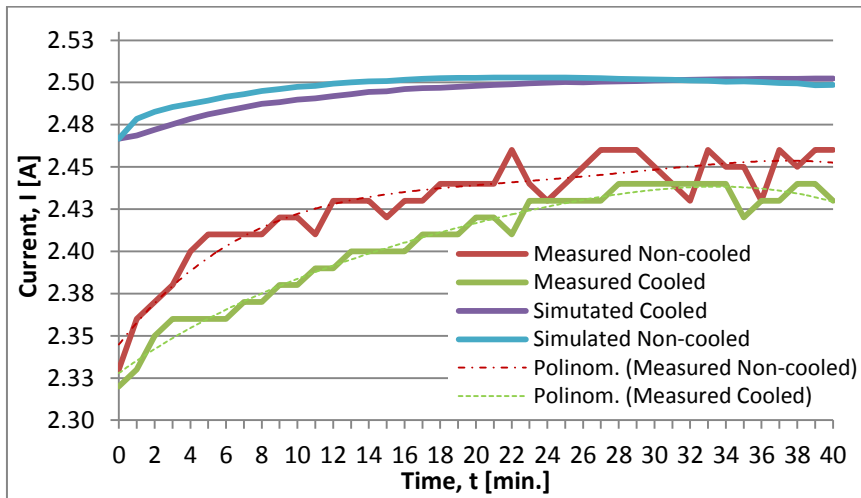
Figure 14
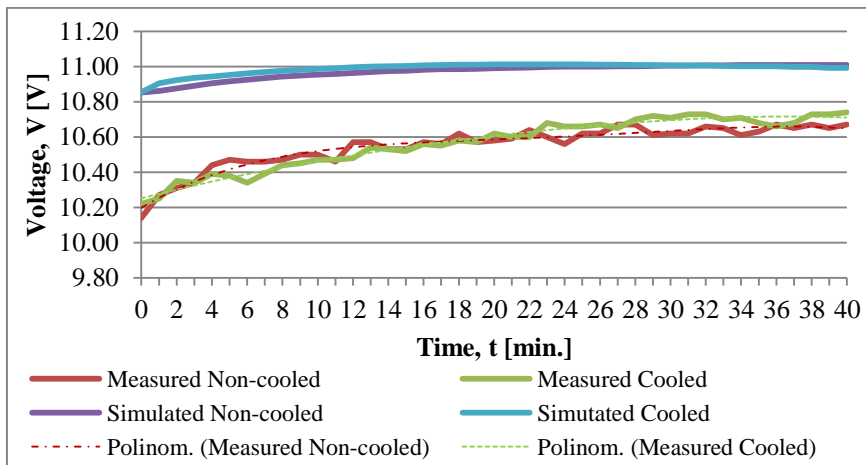The time function of the loaded solar panel's current in chilled and non-cooled cases

Figure 15
The time function of the loaded solar panel's voltage in chilled and non-cooled cases

During the transient analyzation of the loaded solar panel, the results from the measurements approach the simulation results more closely. The curves nature exactness is best seen in terms of power.

Table 6 summarizes the statistical data of differences between simulated and measured results, during transient analyzes in case of loaded solar panel, in both chilled and non-cooled cases. It can be observed that the largest difference between simulation and measurement of power is greater than 10% in both chilled and non-cooled cases. There is no repeat (modus) in the deviations.
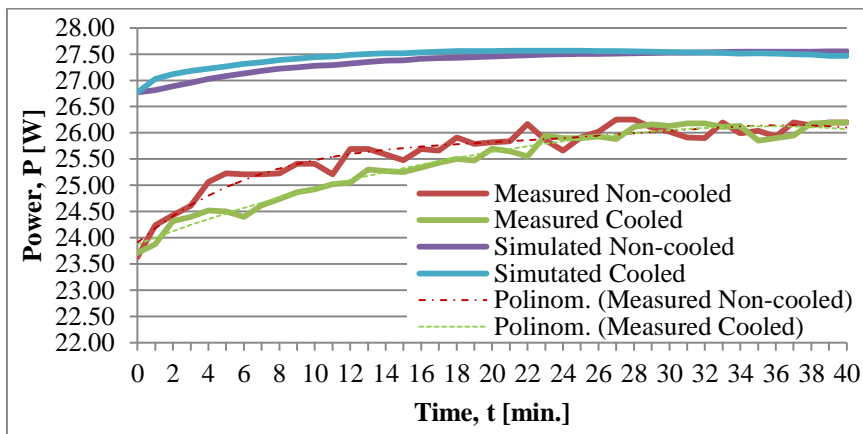
Figure 16

The time function of the loaded solar panel in chilled and non-cooled cases

Table 6

Statistical data of difference between simulated and measured results

	Cooled				Non-cooled			
	Min [%]	Max [%]	Median [%]	Avarage [%]	Min [%]	Max [%]	Median [%]	Avarage [%]
I	1.58	5.87	2.55	2.67	2.40	6.37	3.82	3.58
U	3.11	7.04	3.78	4.00	2.36	6.39	3.90	4.03
P	4.80	11.30	6.34	6.79	4.83	13.18	7.89	8.04

Conclusions

The open circuit voltage and short circuit amperage values were close to the values described in the literature. The measurement results approached the values from the numerical simulation well. In case of the loaded solar panel, during the transient analyzes, the voltage increased, while the current decreased almost the same, due to the temperature decrease. Cooling increased the P_{th} theoretical power. So the main goal of the cooling is to improve the solar panel's energetic efficiency and to increase its lifetime. The results of the experimental and simulation examinations clearly reflect that the cooling changes the solar panel power in a positive direction, so the basic assumption is correct.

After comparing the measurement results with the simulation results, the conclusion can be drawn that the efficiency of the solar panel decreased compared to its new state. However, it should be not be ignored that the results are significantly dependent on the inaccuracy of the instruments and the measurement method, the measurement errors. So, the resulting percentage deviations can also be tracked back to these.

Inaccuracies and many other things may cause the difference between measured and calculated data. The illumination I used, did not reproduce the natural light enough (smaller, and not sufficiently homogeneous light intensity, different wavelength structure). During the aging of the solar panel, efficiency degradation is experienced, which results in a decrease in power.

The manufacturer warrants that the efficiency of the solar panel will not decrease more than 10% in the first 10 years. The solar panel I used during the examinations was 7 years old. The efficiency decrease of the solar panel was about 4%, which was calculated from the simulation and measurement results.

It is important to note that each solar panel manufacturer gives the maximum power and efficiency of the solar panel, measured with STC (Standard Test Conditions). The value of the light intensity is 1,000 W/m^2 in that case, the temperature of solar cells is 25 $°C$ and the value of air density is AM 1.5. These conditions can only be realized in an ideal case. The temperature value differs from those actually experienced. Based on these, it can be said that the power of the solar panel in majority of cases is less than the maximum power given by the manufacturer. During the examinations I made, the lowest cell temperature was about 30$°C$, so it did not meet the STC temperature criteria. This also contributed to the difference between the measured and the maximum power from the catalog. Some manufacturers correct this and give so-called electrical parameter values valid on NOCT (Normal Operating Cell Temperature). These values are closer to the real values. The NOTC means 800W/m^2 light intensity, 20 $°C$ temperature and 1 m/s air flow speed, and the manufacturer gives the temperature value of the module during the operation. This value moves between 33 $°C$ and 58 $°C$ in practice [19, 20, 21].

References

[1]   Hersch, P.: Basic photovoltaic principles and methods. United States Department for Energy. USA, 1982. p. 55

[2]   King, L. D., Kratohvil, A. J., Boyson, E. W.: Temperature Coefficients for PV Modules and Arrays: Measurement Methods, Difficulties, and Results, 26th IEEE Photovoltaic Specialists Conference, Anaheim, California, 1997. pp. 1183-1186

[3]   Dubey, S., Sarvaiya, J. N., Seshadri, B.: Temperature Dependent Photovoltaic (PV) Efficiency and Its Effect on PV Production in the World-A Review. Energy Procedia 33. 2013. pp. 311-321

[4]   Singh, P., Singh, S. N., Lal, M., Husain, M.: Temperature dependence of I-U characteristics and performance parameters of silicon solar cell. Solar Energy Materials and Solar Cells. Vol. 92. No. 12. 2008, pp. 1611-1616

[5]   Szász, Cs.: Optimal control of Photovoltaic Modules Energy Efficiency. Journal of Computer Science and Control Systems. Vol. 10, No. 1, 2017, pp. 29-34

I. Bodnár

Electric Parameters Determination of Solar Panel by Numeric Simulation
and Laboratory Measurements during Temperature Transient

[6]   Zerhouni, Z. F., Zerhouni, H. M., Zegrar, M., Benmesseaoud, T. M., Stambouli, B. A., Midoun, A.: Prosed methods to increase the output efficiency of a photovoltaic (PV) system. Acta Polytechnica Hungarica. Vol. 7, No. 2, 2010, pp. 55-70

[7]   Makhloufi, M. T., Khireddine, M. S., Abdessemed, Y., Boutarafa, A.: Maximum power point tracking of a photovoltaic system using a fuzzy logic controller on DC/DC boost converter. International Journal of Computer Science. Vol. 11, No. 3, 2014, p. 12

[8]   Kádár, P., Varga, A.: Measurement of spectral sensitivity of PV cells. 2012 IEEE 10th Jubilee International Symposium on Intelligent Systems and Informatics. 2012, pp. 549-552

[9]   Chan, D. S. H., Phang, J. C. H.: Analytical methods for the extraction of solar-cell single- and double-diode model parameters from I-V characteristics. IEEETransactions on Electron Drives. Vol. 34, No. 2, 1987, pp. 286-293

[10]   Ishaque, K., Salam, Z., Taheri, H.: Simple, fast and accurate two-diode model for photovoltaic modules. Solar Energy Materials and Solar Cells, Vol. 95, No. 2, 2011, pp. 586-594

[11]   Chegaar, M., Ouennoughi, Z., Hoffmann, A.: A new method for evaluating illuminated solar cell parameters. Solid-State Electronic, Vol. 45, No. 2, 2001. pp. 293-296

[12]   Kurobe, K., Matsunami, H.: New two-diode model for detailed analysis of multicrystalline silicon solar cell. Japanese Journal of Applied Physics, Vol. 44, 2005, pp. 8314-8321

[13]   Ishaque, K., Salam, Z., Taheri, H., Syafaruddin: Modelling and simulation of photovoltaic (PV) system during partial shading based on a two-diode model. Simulation Modelling Practice and Theory, Vol. 19, No. 7, 2011, pp. 1613-1626

[14]   Malik, A. Q., Damit, S. J. B. H., Outdoor testing of single crystal silicon solar cells. Renewable Energy 28, 2003, pp. 1433-1445

[15]   Nagy, D., Rácz, E., Varga, A. Ruf, H., Neuchel, E., R.: Comparison of electric current – voltage, characteristics and maximal power point values of differently and artificially aged solar panels. Proceedings of the 13th IEEE International Symposium on Applied Computational Intelligence and Informatics. 2016, pp. 295-300

[16]   Varga, A., Libor, J., Rácz, E., Kádár, P.: A small laboratory-scale experimental method and arrangement for investigating wavelength dependent irradiation of solar cells. Proceedings of the 11th IEEE International Symposium on Applied Computational Intelligence and Informatics. 2014, pp. 137-141

[17]   Radziemska, E.: The effect of temperature on the power drop in crystalline silicon solar cells. Renewable Energy. Vol. 28, No. 1, 2003. pp. 1-12

[18]   Skoplaki, E., Palyvos, J. A.: On the temperature dependence of photovoltaic module electrical performance: A review of efficiency/power correlations. Solar Energy. Vol. 83, No. 5, 2009, pp. 614-624

[19]   Siddiqui, R., Kumar, R., Jha, K. G., Morampudi, M., Rajput, P., Lata, S., Agariya, S., Nanda, G.,Raghava, S. S.: Comparison of different technologies for solar PV (Photovoltaic) outdoor performance using indoor accelerated aging tests for long term reliability. Energy. Vol. 107, No. 15, 2016, pp. 550-561

[20]   Munoz-Garcia, M. A., Marin, O., Alonso-García, M. C., Chenlo, F.: Characterization of thin film PV modules under standard test conditions: Results of indoor and outdoor measuremnets and the effects of sunlinght exposure. Solar Energy. Vol. 86, No. 10, 2012, pp. 3049-3056

[21]   Földváry, Á.: Napelemeklaboratórium. Budapest University of Technology and Economics. Performance materials. 2015, p. 32

[22]   Precup, R. E., Preitl, S., Korondi, P.: Fuzzy Controllers With Maximum Sensitivity for Servosystems. IEEE Transactions on Industrial Electronics, Vol. 54, No. 3, 2007, pp. 1298-1310

[23]   Ürmös, A., Farkas, Z., Farkas, M., Sándor, T., Kóczy, L.T., Nemcsics, Á.: Application of self-organizing maps for technological support of droplet epitaxy, Acta Polytechnica Hungarica, Vol. 14, No. 4, 2017, pp. 207-224

[24]   Shams, M., Rashedi, E., Dashti, S.M., Hakimi, A.: Ideal gas optimization algorithm. International Journal of Artificial Intelligence. Vol. 15, No. 2, 2017, pp. 116-130

[25]   Pareja-Aparicio, M., Pelegrí-Sebastia, J., Sogorb, T., Llario, V.: Modeling of Photovoltaic Cell Using Free SoftwareApplication for Training and Design Circuit inPhotovoltaic Solar Energy. INTECH World's largest Science,Technology & MedicineOpen Access book publisher. Chapter 6, 2013, p. 21

[26]   Kandil, M. K., Altouq, M. S., Al-asaad, A. M., Alshamari, L. M., Kadad, I. M., Ghoneim, A. A.: Investigation of the Performance of CIS Photovoltaic Modules under Different Environmental Conditions. Smart Grid and - Renewable Energy. No. 2, 2011, pp. 375-387

[27]   Mishima, T., Taguchi, M., Sakata, H., Maruyama, E.: Development status of high-efficinecy HIT solar cells. Solar Energy Materials and Solar Cells. Vol. 95, 2011, pp. 18-21

[28]   Singh, P., Ravindra, N.M.: Temperature dependence of solar cell performance – an analysis. Solar Energy Materials and Solar Cells. Vol. 101, 2012, pp. 36-45

I. Bodnár

Electric Parameters Determination of Solar Panel by Numeric Simulation
and Laboratory Measurements during Temperature Transient

[29] Chantana, J., Kato, T., Sugimoto, H., Minemoto T.: Time-resolved photoluminescence of Cu(In,Ga)(Se,S)2 thin films and temperature dependent current density-voltage characteristics of their solar cells on surface treatment effect. Current Applied Physics. Vol. 17, No. 4, 2017, pp. 461-466

[30] Ashi, S., Teranishi., H., Kusaki, K., Kaizu, T., Kita, T.: Two-step photon up-conversion solar cell. Nature Communitacions. 2017, p. 9

[31] Malik, A. Q., Ming, L. C., Sheng, T. K., Blundel, M.: Influence of Temperature on the Performance of Photovoltaic Polycrystalline Silicon Module in the Bruneian Climate. AJSTD Vol. 26, No. 2, 2010, pp. 61-72

[32] Yadav, P., Pandey, K., Bhatt, V., Kumar, M., Kim, J.: Critical aspects of impedance spectroscopy in silicon solar cell characterization: A review. Renewable and Sustainable Energy Reviews. Vol. 76, 2017, pp. 1562-1578

[33] Altermatt, P., Reinders, A., Verlinden, P., van Sark W.,Freundlich A.: Numerical Simulation of Crystalline Silicon Solar Cells. Photovoltaic Solar Energy. 2017, p. 682

[34] Sundarabalan, C. K., Selvi, K., Sakeenathul Kubra, K.: Performance Investigation of Fuzzy Logic Controlled MPPT for Energy Efficient Solar PV Systems.Power Electronics and Renewable Energy Systems. Vol. 326, 2014, pp. 761-770

[35] Verma, D., Nema, S., Shandilya, A. M., Soubhagya Dash, K.: Maximum power point tracking (MPPT) techniques: Recapitulation in solar photovoltaic systems. Renewable and Sustainable Energy Reviews. Vol. 54, 2016, pp. 1018-1034

[36] Gobhinat, S., Ram Abhinav, P. S., Gowtham, V., Lokesh, S.: A Prototype Development of MPPT Algorithm based Solar Photovoltaic Charging System. International Journal of Engineering and Management Research (IJEMR). Vol. 6, No. 2, 2016, 139-143

[37] Guo, J., Lin, S., Bilbao, J. I., White, S. D., Sproul, A. B.: A review of photovoltaic thermal (PV/T) heat utilisation with low temperature desiccant cooling and dehumidification. Renewable and Sustainable Energy Reviews. Vol. 67, 2017, pp. 1-14

[38] Farshchimonfared, M., Bilbao, J. I., Sproul, A. B.: Full optimisation and sensitivity analysis of a photovoltaic–thermal (PV/T) air system linked to a typical residential building. Solar Energy. Vol. 136, 2016, 15-22

[39] Koós, D., Szaszák, N., Bodnár, I., Boldizsár, Cs.: Temperature Dependance of Solar Cell's. ActaTechnicaCorviniensis- Bulletin of Engineering. Vol. 9, No. 2, 2016, pp. 107-110